JACS
JOURNAL OF THE AMERICAN CHEMICAL SOCIETY

Communication

pubs.acs.org/JACS

Aligned 1-D Nanorods of a π-Gelator Exhibit Molecular Orientation and Excitation Energy Transport Different from Entangled Fiber Networks

Keita Sakakibara,[†] Parayalil Chithra,[†] Bidisa Das,[∥] Taizo Mori,[†] Misaho Akada,[†] Jan Labuta,[†] Tohru Tsuruoka,*[,†] Subrata Maji,[∥] Seiichi Furumi,[‡] Lok Kumar Shrestha,[†] Jonathan P. Hill,[†] Somobrata Acharya,*[,∥] Katsuhiko Ariga,*[,†] and Ayyappanpillai Ajayaghosh*[,§]

[†]World Premier International (WPI) Research Center for Materials Nanoarchitectonics (MANA), National Institute for Materials Science (NIMS), 1-1 Namiki, Tsukuba, Ibaraki 3050044, Japan

[∥]Centre for Advanced Materials (CAM), Indian Association for the Cultivation of Science, Kolkata 700032, India

[‡]Applied Photonic Materials Group, National Institute for Materials Science (NIMS), 1-2-1 Sengen, Tsukuba, Ibaraki 3050047, Japan

[§]Photosciences and Photonics Group, Chemical Sciences and Technology Division, Council of Scientific and Industrial Research—National Institute for Interdisciplinary Science and Technology (CSIR-NIIST), Trivandrum 695019, India

Supporting Information

ABSTRACT: Linear π-gelators self-assemble into entangled fibers in which the molecules are arranged perpendicular to the fiber long axis. However, orientation of gelator molecules in a direction parallel to the long axes of the one-dimensional (1-D) structures remains challenging. Herein we demonstrate that, at the air−water interface, an oligo(*p*-phenylenevinylene)-derived π-gelator forms aligned nanorods of 340 ± 120 nm length and 34 ± 5 nm width, in which the gelator molecules are reoriented parallel to the long axis of the rods. The orientation change of the molecules results in distinct excited-state properties upon local photoexcitation, as evidenced by near-field scanning optical microscopy. A detailed understanding of the mechanism by which excitation energy migrates through these 1-D molecular assemblies might help in the design of supramolecular structures with improved charge-transport properties.

In supramolecular assemblies of chromophoric systems, the mode of packing of molecules at the nanoscale is a critical factor that controls the excited-state photophysical and energy-transport processes.[1,2] Therefore, control of long-range molecular order that determines the excitation delocalization and relaxation pathways is central to the design of artificial light-harvesting systems with synthetic molecular assemblies.[1c,2] Generally, in the case of π-systems, design of one-dimensional (1-D) fibers with chromophores oriented perpendicular to the long axis[3] is relatively easy due to the spontaneous π-stacking of the molecules. However, changing the orientation of the same chromophores from a perpendicular to a parallel configuration relative to the fiber long axis remains extremely challenging.[4] This is particularly true for π-gelators, which form entangled networks of 1-D fibers with chromophores packed perpendicular to the long fiber axis.[5] While kinetic and thermodynamic aspects of the supramolecular polymerization of π-systems are well understood,[1g,6,7] molecular orientational control of the excited-state properties of such supramolecular polymers remains relatively unexplored. A deeper understanding of both the mechanistic aspects and the excited-state properties of π-system-based self-assemblies is of great importance for optimizing the performance of electronic and photonic devices.

Herein we report the fabrication of aligned 1-D nanorods of a π-gelator in which the molecules are organized parallel to the long axis, in contrast to the usual perpendicular orientation in entangled fiber assemblies. The oligo(*p*-phenylenevinylene)-derived π-gelator OPV-**1** (Figure 1A), a well-known organogelator,[8] is known to form an entangled network of supramolecular fibers (Figure 1B) in which the OPV-**1** molecules are arranged perpendicular to the fiber long axis

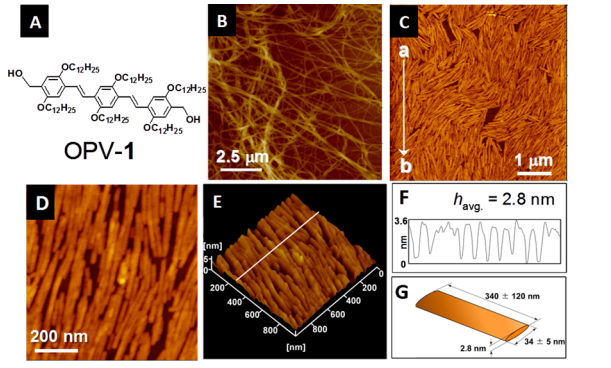

Figure 1. (A) Chemical structure of OPV-**1**. (B) AFM image of the self-assembled chaotic fibers of OPV-**1** upon drop-casting from toluene solution. (C,D) AFM images of OPV-**1** aligned rods on freshly cleaved mica surface formed at π = 0 mN m^{-1} (arrow a→b in image C indicates the dipping direction of LB films). (E) 3-D height profile of the rods at π = 5 mN m^{-1}. (F) Height profile along the white line in panel E. (G) Schematic of an individual rod showing its dimensions, ~340 × 34 × 2.8 nm^3.

Received: April 22, 2014
Published: May 29, 2014

   dx.doi.org/10.1021/ja504014k | *J. Am. Chem. Soc.* 2014, 136, 8548−8551

upon drop-casting from a toluene solution. Interestingly, spreading a homogeneous solution of OPV-**1** in chloroform onto the air−water interface of a Langmuir trough resulted in the formation of aligned supramolecular rods, as evident from the atomic force microscopy (AFM) imaging (Figure 1C−E and Supporting Information, Figure S4). For example, at surface pressure (π) = 0 mN m^{-1}, non-collapsed and non-entangled short rods were observed (Figures 1C,D and S1−S3). These rods gradually aligned parallel to the barrier upon increasing the surface pressure to π = 5 mN m^{-1} (Figures 1E and S4C), became more densely packed at π = 30 mN m^{-1}, and were agglomerated at π = 55 mN m^{-1} (Figure S4D−G). Evidently, increases in surface pressure effectively fill voids in the monolayer film and align the rods in one direction. Cross-sectional analysis (Figure 1E,F) indicates rods with uniform height (2.8 ± 0.5 nm), width (34 ± 5 nm), and length (340 ± 120 nm) (Figure 1G). The temperature of the water subphase does not affect the characteristics of the rod formation (Figure S5). Formation of aligned rods of OPV-**1** gelators is surprising, since chaotic 1-D fibers of OPV gelators are commonly found due to their spontaneous self-assembly in solution.

We studied the molecular orientation within the aligned rods formed at the air−water interface using far-field polarized optical spectroscopy. The polarized UV−visible spectra showed an absorption peak at 407 nm with enhanced intensity for the parallel polarization ($OD_{\parallel}$) compared to the perpendicular polarization ($OD_{\perp}$), with significant anisotropy ($OD_{\parallel}/OD_{\perp}$) of 2.0 (Figure S6). The angular dependence of transition dipole moment is recorded using the dichroic relation, which reveals a tilt angle of 51° for the transition dipoles with respect to the substrate normal (Figure S7). The 2.8 nm thicknesses of individual rods obtained by AFM and molecular tilt of 51° together indicate a slanted molecular orientation within the rods (Figure S8). Polarized fluorescence spectra of the aligned rods exhibit significant anisotropy, with polarization intensity ratio ($I_{\parallel}/I_{\perp}$) of 2.4 (Figure 2A), where $I_{\parallel}$ and $I_{\perp}$ are the spectral intensities parallel and perpendicular to the long axis of the rods, respectively. This observation is in contrast to the previous fluorescence polarization measurements on entangled fibers of OPV-**1** gel upon alignment, which showed stronger fluorescence intensity in the perpendicular direction (Figure 2C).[3c] Additionally, we carried out polarization-angle-resolved fluorescence spectroscopy to confirm the molecular orientation within the rods (Figures 2B, S9, and S10). The emission band at 530 nm is strongly polarized in a direction parallel to the aligned fibers and exhibits a modulation of emission intensity with polarization angle. The polarization ratio (r) was calculated as 0.66 from the intensity ratio, $r = (I_{\parallel} - I_{\perp})/(I_{\parallel} + I_{\perp})$, versus detection angle, while the plot was fitted with a sine square function.

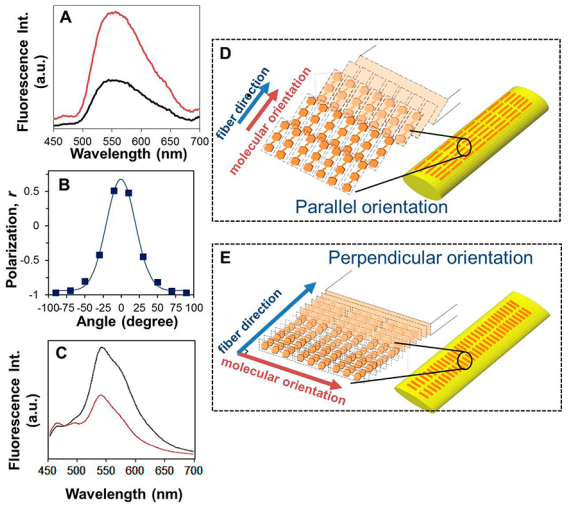

Figure 2. (A) Polarized fluorescence spectra and (B) polarization ratio (r) versus detection angle for the LB-aligned rods. (C) Polarized fluorescence spectra of entangled fibers aligned in a narrow cuvette (0.1 mm thickness). Spectra were recorded with parallel (red) and perpendicular (black) polarized light against the alignment direction. (D,E) Schematic illustrations of molecular assembly of OPV-**1** in aligned rods and entangled fibers, respectively.

The polarization ratio reflects a high degree of alignment of the OPV-**1** molecules with orientation parallel to the long axis of the aligned rods (Figure 2D), which is different from that of the entangled gel fiber network, where OPV-**1** molecules stack in lamellae with their molecular long axes perpendicular to the long axis of the fibers (Figure 2C,E).[3c,9] Thus, the air−water interface enables reorientation of OPV-**1** molecules from the conventional perpendicular (90°) to an unconventional parallel (0°) arrangement, with the molecular axis lying parallel to the long axis of the rods. This situation may arise from the possibility that the initially formed OPV-**1** tapes at the air−water interface roll up in the direction opposite to the direction of molecular orientation on application of pressure, resulting in rods that will minimize the contact of the alkyl chains with water. In this rolling process, the width of the tapes becomes the length of the rods, and the molecular orientation becomes parallel to the long axis of the latter. Thus, the direction of the molecular arrangements changes without disturbing the molecular packing, which is clear from the identical film X-ray diffraction patterns of the entangled fibers and the aligned rods.

Excitation energy transfer in the entangled fibers[2a,e,10] and aligned rods was visualized using near-field photoluminescence (PL) and topographic imaging (Figure S11) using near-field scanning optical microscopy (NSOM).[11] Correlation of the local NSOM topography with the fluorescence reveals that orthogonal phasing of OPV-**1** orientation contributes significantly to the excitation migration behavior in the rods (Figure 3). Excitation of a fiber in the entangled network resulted in fluorescence along the fibers (Figure 3A), which is in agreement with our previous observation of fast excitation energy migration and energy transfer in OPV gel fibers.[10] In

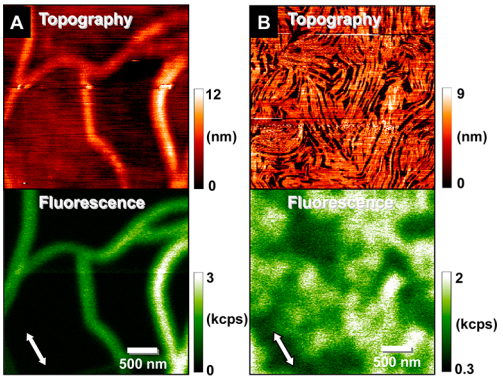

Figure 3. Surface topography (top images) and fluorescence NSOM (bottom images) of (A) OPV-**1** assemblies prepared by drop-casting from toluene solution and (B) LB film formed at π = 5 mN m^{-1}.

dx.doi.org/10.1021/ja504014k | J. Am. Chem. Soc. 2014, 136, 8548−8551

contrast, the aligned rods exhibit a modulation of fluorescence along the individual rods as well as between the closely packed rods (Figure 3B). When the aligned rods were excited, localized regions of fluorescence were observed. LB films prepared at different surface pressures exhibit similar behavior, revealing an identical excitation migration mechanism within the aligned rods (Figures S12 and S13). Repetitive measurements revealed comparable fluorescence intensities from strongly fluorescent regions within the aligned rods, while entangled fibers exhibited variable intensities among different fibers (Figure S14).

Polarized fluorescence mapping of individual aligned rods revealed a correlation between the topographic angle and its corresponding fluorescence (Figure 4A,B). Rods aligned parallel to the y-axis of the image frame tend to exhibit stronger fluorescence than those inclined at an angle to the y-axis, resulting in modulation of the fluorescence intensity at the macroscopic scale (Figure 4B). While intra-chain energy migration is efficient in the entangled gel fibers, aligned rods with parallel arrangement of OPV-**1** reveal inter- versus intra-rod excitation migration processes. Confirmation for the inter-rod excitation energy transfer was obtained by measuring the fluorescence intensities from a discrete set of neighboring parallel rods (Figure 4C). Excitation of the n^{th} rod in the aligned assembly results in fluorescence distribution among the $n \pm i$ rods, where i represents the number of neighboring rods on either side of the n^{th} rod. The intensity of the fluorescence depends on the strength of the rod-coupling, which in turn depends on the packing within the aligned assembly. The fluorescence intensity apparently increases when the inter-rod distance is less than ca. 70 nm, indicating occurrence of excitation migration processes among the adjacent rods (Figure 4D).

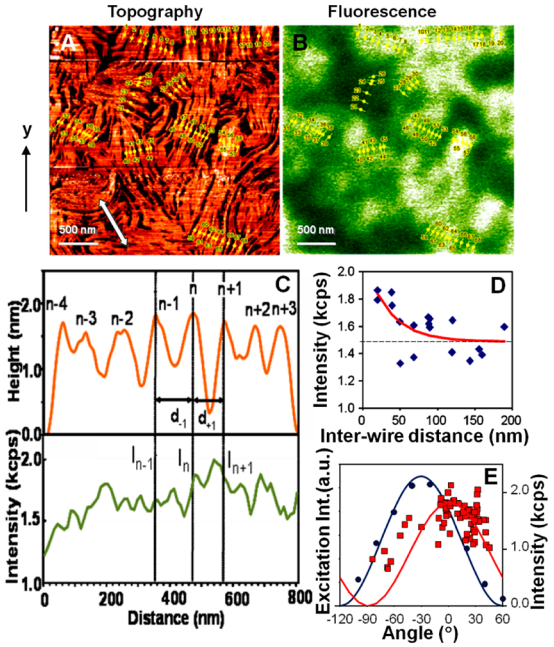

Figure 4. (A) NSOM topography and (B) fluorescence images of the aligned rods prepared at π = 5 mN m^{-1}. Sixty-eight individual rods were monitored for angle-resolved polarization (yellow marks). The arrow in panel A indicates the direction of polarization. Corresponding 30° deviation can be seen in panel E. (C) Plot of fiber height profile and fluorescence intensity versus distance on either side of excitation. Each point for the height profile of the fibers was defined from the topographic height profile in panel A, and the fluorescence intensity at each point was collected from panel B. (D) Plot of the fluorescence intensity as a function of the distance between individual fibers. The solid red line represents nonlinear least-squares fits of the exponential decay. (E) Angle dependence of the NSOM excitation source and the fluorescence from individual fibers. Power intensity of a He-Cd laser (325.0 nm) is shown as a function of the angle (blue dots and solid line shows fit of Malus' law). Fluorescence intensity of individual fibers is shown as a function of the angle between the major axis of the fiber and the vertical y-axis within the detection plane (red squares and solid line shows fit of Malus' law).

In addition, the angular dependence of excitation energy migration is further supported by correlating the intensity of the polarized excitation source with the fluorescence intensities of individual rods within the assembly (Figure 4E). Both the excitation source and the fluorescence intensity from individual rods show intensity variation following Malus' law[12] (Figure 4E), suggesting that the excitation energy transfer from one OPV-**1** to another takes place on a time scale faster than a new equilibrium position of neighboring OPV-**1** molecules can be established.

In summary, at the air−water interface, OPV-**1** self-assembles to form nanorods with molecules arranged parallel to the length of the rods, in contrast to the usual perpendicular arrangement in the entangled gel network fibers. Long-range excitation energy transfer occurs in the entangled fibers with significant fluorescence quenching, while large fluorescence enhancement occurs in the aligned nanorods. Thus, entangled gel fibers having perpendicular arrangement of molecules are more suitable for excitation energy transfer, while the nanorods possessing parallel arrangement of molecules may be better suited for charge transport. These findings emphasize the importance of understanding the molecular organization and nanoscopic morphology of self-assembled architectures to control the excited-state properties, which may be useful for their efficient sensing and imaging applications.

■ ASSOCIATED CONTENT

Ⓢ Supporting Information

Experimental details and additional figures and data. This material is available free of charge via the Internet at http://pubs.acs.org.

■ AUTHOR INFORMATION

Corresponding Authors

tsuruoka.tohru@nims.go.jp
camsa2@iacs.res.in
ariga.katsuhiko@nims.go.jp
ajayaghosh@niist.res.in

Notes

The authors declare no competing financial interest.

■ ACKNOWLEDGMENTS

This work was supported by WPI-MANA, MEXT, and CREST program of JST, Japan. We thank G. Villora (NIMS) for polarized fluorescent measurements. A.A. is grateful to Department of Atomic Energy, Govt. India, for an Outstanding Researcher Award, and S.A. acknowledges DST and CSIR, Govt. India, for financial support.

■ REFERENCES

(1) (a) Hoeben, F. J. M.; Jonkheijm, P.; Meijer, E. W.; Schenning, A. P. H. J. *Chem. Rev.* **2005**, *105*, 1491. (b) Chen, Z. J.; Lohr, A.; Saha-

Müller, C. R.; Würthner, F. *Chem. Soc. Rev.* **2009**, *38*, 564. (c) Babu, S. S.; Kartha, K. K.; Ajayaghosh, A. *J. Phys. Chem. Lett.* **2010**, *1*, 3413. (d) Hong, Y.; Lam, J. W. Y.; Tang, B. Z. *Chem. Soc. Rev.* **2011**, *40*, 5361. (e) An, B.-K.; Gierschner, J.; Park, S. Y. *Acc. Chem. Res.* **2012**, *45*, 544. (f) Tovar, J. D. *Acc. Chem. Res.* **2013**, *46*, 1527. (g) Korevaar, P. A.; De Greef, T. F. A.; Meijer, E. W. *Chem. Mater.* **2014**, *26*, 576.

(2) (a) Ajayaghosh, A.; Praveen, V. K.; Vijayakumar, C. *Chem. Soc. Rev.* **2008**, *37*, 109. (b) Würthner, F.; Kaiser, T. E.; Saha-Möller, C. R. *Angew. Chem., Int. Ed.* **2011**, *50*, 3376. (c) Maggini, L.; Bonifazi, D. *Chem. Soc. Rev.* **2012**, *41*, 211. (d) Praveen, V. K.; Ranjith, C.; Armaroli, N. *Angew. Chem., Int. Ed.* **2014**, *53*, 365. (e) Praveen, V. K.; Ranjith, C.; Bandini, E.; Ajayaghosh, A.; Armaroli, N. *Chem. Soc. Rev.* **2014**, *43*, 4222.

(3) (a) Wu, Z.; Wu, S.; Liang, Y. *Langmuir* **2001**, *17*, 7267. (b) Jeukens, C. R. L. P. N.; Jonkheijm, P.; Wijnen, F. J. P.; Gielen, J. C.; Christianen, P. C. M.; Schenning, A. P. H. J.; Meijer, E. W.; Maan, J. C. *J. Am. Chem. Soc.* **2005**, *127*, 8280. (c) Hirai, Y.; Babu, S. S.; Praveen, V. K.; Yasuda, T.; Ajayaghosh, A.; Kato, T. *Adv. Mater.* **2009**, *21*, 4029. (d) Rao, K. V.; Jayaramulu, K.; Maji, T. K.; George, S. J. *Angew. Chem., Int. Ed.* **2010**, *49*, 4218. (e) Giansante, C.; Raffy, G.; Schafer, C.; Rahma, H.; Kao, M. T.; Olive, A. G. L.; Del Guerzo, A. *J. Am. Chem. Soc.* **2011**, *133*, 316. (f) Wall, B. D.; Diegelmann, S. R.; Zhang, S.; Dawidczyk, T. J.; Wilson, W. L.; Katz, H. E.; Mao, H.-Q.; Tovar, J. D. *Adv. Mater.* **2011**, *23*, 5009.

(4) (a) Würthner, F.; Yao, S.; Beginn, U. *Angew. Chem., Int. Ed.* **2003**, *42*, 3247. (b) Yao, S.; Beginn, U.; Gress, T.; Lysetska, M.; Würthner, F. *J. Am. Chem. Soc.* **2004**, *126*, 8336. (c) Kaiser, T. E.; Stepanenko, V.; Würthner, F. *J. Am. Chem. Soc.* **2009**, *131*, 6719. (d) Schmidt, R.; Stolte, M.; Grüne, M.; Würthner, F. *Macromolecules* **2011**, *44*, 3766.

(5) Babu, S. S.; Praveen, V. K.; Ajayaghosh, A. *Chem. Rev.* **2014**, *114*, 1973.

(6) (a) Jonkheijm, P.; van der Schoot, P.; Schenning, A. P. H. J.; Meijer, E. W. *Science* **2006**, *313*, 80. (b) Korevaar, P. A.; George, S. J.; Markvoort, A. J.; Smulders, M. M. J.; Hilbers, P. A. J.; Schenning, A. P. H. J.; De Greef, T. F. A.; Meijer, E. W. *Nature* **2012**, *481*, 492. (c) Korevaar, P. A.; Grenier, C.; Markvoort, A. J.; Schenning, A. P. H. J.; De Greef, T. F. A.; Meijer, E. W. *Proc. Natl. Acad. Sci. U.S.A.* **2013**, *110*, 17205.

(7) (a) García, F.; Sánchez, L. *J. Am. Chem. Soc.* **2012**, *134*, 734. (b) Mayoral, M. J.; Rest, C.; Stepanenko, V.; Schellheimer, J.; Albuquerque, R. Q.; Fernández, G. *J. Am. Chem. Soc.* **2013**, *135*, 2148. (c) Ogi, S.; Sugiyasu, K.; Manna, S.; Samitsu, S.; Takeuchi, M. *Nat. Chem.* **2014**, *6*, 188.

(8) (a) Ajayaghosh, A.; George, S. J. *J. Am. Chem. Soc.* **2001**, *123*, 5148. (b) George, S. J.; Ajayaghosh, A. *Chem.—Eur. J.* **2005**, *11*, 3217. (c) Ajayaghosh, A.; Praveen, V. K. *Acc. Chem. Res.* **2007**, *40*, 644.

(9) (a) van Herrikhuyzen, J.; George, S. J.; Vos, M. R. J.; Sommerdijk, N. A. J. M.; Ajayaghosh, A.; Meskers, S. C. J.; Schenning, A. P. H. J. *Angew. Chem., Int. Ed.* **2007**, *46*, 1825. (b) Kumar, V. R. R.; Sajini, V.; Sreeprasad, T. S.; Praveen, V. K.; Ajayaghosh, A.; Pradeep, T. *Chem.—Asian J.* **2009**, *4*, 840.

(10) (a) Ajayaghosh, A.; Vijayakumar, C.; Praveen, V. K.; Babu, S. S.; Varghese, R. *J. Am. Chem. Soc.* **2006**, *128*, 7174. (b) Ajayaghosh, A.; Praveen, V. K.; Vijayakumar, C.; George, S. J. *Angew. Chem., Int. Ed.* **2007**, *46*, 6260. (c) Vijayakumar, C.; Praveen, V. K.; Ajayaghosh, A. *Adv. Mater.* **2009**, *21*, 2059. (d) Vijayakumar, C.; Praveen, V. K.; Kartha, K. K.; Ajayaghosh, A. *Phys. Chem. Chem. Phys.* **2011**, *13*, 4942.

(11) (a) Vanden Bout, D. A.; Kerimo, J.; Higgins, D. A.; Barbara, P. F. *Acc. Chem. Res.* **1997**, *30*, 204. (b) Eisele, D. M.; Knoester, J.; Kirstein, S.; Rabe, J. P.; Vanden Bout, D. A. *Nat. Nanotechnol.* **2009**, *4*, 658.

(12) (a) Beermann, J.; Bozhevolnyi, S. I.; Balzer, F.; Rubahn, H.-G. *Laser Phys. Lett.* **2005**, *10*, 480. (b) Balzer, F.; Beermann, J.; Bozhevolnyi, S. I.; Simonsen, A. C.; Rubahn, H.-G. *Nano Lett.* **2003**, *3*, 1311.